

See discussions, stats, and author profiles for this publication at: <https://www.researchgate.net/publication/272825380>

Solvatochromic Fluorescent BODIPY Derivative as Imaging Agent in Camptothecin Loaded Hexosomes for Possible Theranostic Applications

Article in RSC Advances · February 2015

DOI: 10.1039/C5RA01025J

CITATION

1

READS

61

11 authors, including:



Claudia Caltagirone

Università degli studi di Cagliari

79 PUBLICATIONS 2,134 CITATIONS

SEE PROFILE



Angela Maria Falchi

Università degli studi di Cagliari

60 PUBLICATIONS 788 CITATIONS

SEE PROFILE



Maura Monduzzi

Università degli studi di Cagliari

167 PUBLICATIONS 3,332 CITATIONS

SEE PROFILE



Antonella Rosa

Università degli studi di Cagliari

92 PUBLICATIONS 1,057 CITATIONS

SEE PROFILE

Electronic Supporting Information

**Solvatochromic Fluorescent Py-BODIPY as imaging agent in Camptothecin Loaded
Hexosomes for Theranostic Applications**

*Claudia Caltagirone, Massimiliano Arca, Angela M. Falchi, Vito Lippolis, Valeria Meli, Maura
Monduzzi, Tommy Nylander, Antonella Rosa, Judith Schmidt, Yeshayahu Talmon and Sergio
Murgia*

Materials and Methods

Chemicals

Monoolein (MO, 1-monooleoylglycerol, RYLO MG 19 PHARMA, glycerol monooleate; 98.1 wt %) was kindly provided by Danisco A/S, DK-7200, Grinsted, Denmark. Pluronic F108 (PEO₁₃₂-PPO₅₀-PEO₁₃₂), oleic acid (OA, 99%), folic acid ($\geq 97\%$), camptothecin ($\geq 90\%$), 1-pyrenecarboxaldehyde (99%), pyrrole (98%), 2,3-dichloro-5,6-dicyano-1,4-benzoquinone (98%), boron trifluoride diethyl etherate (BF₃·Et₂O, $\geq 46.5\%$), triethylamine ($\geq 46.5\%$), trifluoroacetic acid (99%), hexane ($\geq 95\%$), ethyl acetate ($\geq 99.5\%$), dichloromethane (DCM, $\geq 99.9\%$), were purchased from Sigma-Aldrich. Distilled water passed through a Milli-Q water purification system (Millipore) was used to prepare the samples.

Synthesis of 5,5-difluoro-10-(pyren-1-yl)-5H-dipyrrolo[1,2-c:1',2'-f][1,3,2]diazaborinin-4-ium-5-uide (Py-BODIPY)

To a solution of 1-pyrenecarboxaldehyde (1.52 g, 6.6 mmol) in pyrrole (10 mL, 144 mmol) 0.56 mL of trifluoroacetic acid were added under N₂ atmosphere. The resulting dark red mixture was stirred at room temperature for 2h. The desired compound (2,2'-(pyren-1-ylmethylene)bis(1H-pyrrole), **1**) was obtained as a dark green solid after purification by flash chromatography using hexane/ethyl acetate 4:1 (v/v) as eluent. **1** (0.30 g, 0.86 mmol) was then dissolved on DCM (100 mL) and 2,3-dichloro-5,6-dicyano-1,4-benzoquinone (0.23 g, 1.03 mmol) was added at room temperature under N₂ atmosphere. After 30 min triethylamine (4.75 mL, 34.4 mmol) and BF₃·Et₂O were added and the reaction mixture was stirred at room temperature for one hour. Purification by flash chromatography (hexane/ethyl acetate 2:1 v/v as eluent) afforded the desired product as a dark green solid (0.13 g, 0.33 mmol). Yield = 38%. Mp: 135 °C. ¹H-NMR (400 MHz, CDCl₃): δ 6.44-6.53 (m, 2H), 6.60-6.68 (m, 2H), 7.95-8.35 (m, 11H). ¹³C-NMR (400 MHz, CDCl₃): δ 118.90, 119.09, 124.13, 124.39, 124.72, 125.11, 125.38, 126.09, 126.31, 126.78, 127.29, 127.97, 128.66,

129.13, 130.55, 130.89, 131.44, 131.87, 132.67, 136.66, 144.57, 146.65. IR (solid state, cm^{-1}) ν = 1552 (s), 1410 (m), 1376 (s), 1354 (m), 1254 (s), 1102 (s), 1065 (s), 1036 (s), 982 (s).

QM Calculations

Quantum chemical DFT calculations were performed with the commercial suite of software Gaussian09 (rev. A02)¹ on the Py-BODIPY at Density Functional Theory (DFT) level. All calculations adopted the parameter-free PBE0 functional² (implemented as PBE1PBE in Gaussian),³ combining the so-called PBE generalized gradient functional with a predefined amount of exact exchange. For all atomic species the 6-31+G(d,p) basis sets were used. Tight SCF convergence criteria (SCF = tight keyword) and fine numerical integration grids [Integral(FineGrid) keyword] were used and the nature of the minima of each optimized structure was verified by harmonic frequency calculations (freq = raman keyword). The metric parameters optimised in the gas phase (Fig. 8 and Table S1) perfectly match the crystallographic data reported by Ziesel and co-workers.⁴ An almost orthogonal geometry (69.05°) between the mean plane of the indacene fragment and the pyrene subunit was calculated, according to what reported for 4,4-difluoro-8-pyrenyl-1,3,5,7-tetramethyl-2,6-dithyl-1,4-bora-3a,4a-diaza-*s*-indacene (78.00°).⁴ A potential energy scan (PES) was performed by imposing the rotation τ of the pyrenyl ring (τ between 20° and 160° , steps of 5°) and optimizing the resulting geometry at each rotational step (opt = modredundant keyword). The potential energy scan shows that the rotation of the pyrenyl substituent (τ) at the C8 position of the 3a,4a-diaza-*s*-indacene moiety can occur without significantly affecting the total electronic energy of the system (a variation of about 3 kcal mol^{-1} is calculated for $40^\circ \leq \tau \leq 140^\circ$; Fig. S2).

Also the structure featuring the pyrenyl ring perpendicular ($\tau = 90^\circ$) to the BODIPY moiety was separately optimised. Electronic transition energies and oscillator strengths were calculated at the TDDFT level (100 states). The electronic spectra were simulated by a convolution of Gaussian functions centered at the calculated excitation energies (halfbandwidth 0.1 eV). In order to keep into

account the influence of the solvent on the spectroscopic properties of the model compounds, calculations were also carried out in the presence of different solvents, implicitly taken into account by means of the polarizable continuum model approach (linear response; non-equilibrium solvation) in its integral equation formalism variant (IEF-PCM), which describes the cavity of the solute within the reaction field (SCRF) through a set of overlapping spheres.⁵ The programs Molden 5.0⁶ and GaussView 5⁷ were used to investigate the molecular orbital shapes and simulate excitation spectra.

Sample preparation

Monoolein-based hexosomes were prepared and stabilized by dispersing the appropriate amount of MO and oleic acid in water solutions of a 80/20 mixture of Pluronic F108 and folate-conjugated Pluronic F108 (PF108/PF108-FA) using an ultrasonic processor UP100H by Dr. Hielscher, cycle 0.9, amplitude 90 %, for 15 min. Doped hexosomes were obtained by dispersing the drug and the fluorophore in the melted monoolein with the help of an ultrasonic bath before mixing with the Pluronic solution. The sample volume was usually 4 mL with approximately 96.4 wt % of water, 2.97 wt % of MO, 0.33 wt % of OA and 0.3 wt % of Pluronics mixture. Camptothecin and Py-BODIY percentage were respectively 4.3×10^{-4} wt % and 1.48×10^{-3} wt %.

Dialysis and dye and drug loading efficiency

After loading with camptothecin and Py-BODIPY, the hexosome dispersion was purified from the non-encapsulated drug and fluorophore by dialysis: 2 mL were loaded into a dialysis tubing cellulose membrane (14 kDa MW cutoff) and dialyzed against water (1000 mL), for 2 h (by replacing the water after 1 hour). The loading efficiency ($E\%$), expressed as percentage of the amount of the drug and the dye present in the formulation before dialysis, was determined by UV-vis spectroscopy after disruption of hexosomes with acetonitrile. Camptothecin and Py-BODIPY

content were quantified by a Thermo Nicolet Evolution 300 UV-VIS spectrophotometer at 363 and 501 nm respectively for drug and fluorophore.

Cryogenic Transmission Electron Microscopy

Cryogenic transmission electron microscopy (cryo-TEM) experiments were performed to visualize the hexosome nanoparticles. Vitrified specimens were prepared in a controlled environment vitrification system (CEVS) at 25 °C and 100 % relative humidity. A drop (~ 3 μ L) of the sample was placed on a perforated carbon film-coated copper grid, blotted with filter paper, and plunged into liquid ethane at its freezing point. The vitrified specimens were transferred to a 626 Gatan cryo-holder and observed at 120 kV acceleration voltage in an FEI Tecnai T12 G² transmission electron microscope at about -175 °C in the low-dose imaging mode to minimize electron-beam radiation-damage. Images were digitally recorded with a Gatan US1000 high-resolution CCD camera.

Dynamic Light Scattering

For the determination of the size as well as the ζ -potential of the nanoparticles, dynamic light scattering (DLS) and electrophoretic mobility measurements, respectively, were performed at 25 (\pm 0.1) °C using ZetaSizer Nano ZSP (Malvern Instruments Ltd., Worshestershire, U.K.), which is equipped with a 10 mW helium-neon laser (operating at a wavelength of 633 nm). With this instrument, the DLS measurements are carried out at a fixed scattering angle $\theta = 173^\circ$ using a backscattering technique. The electrophoretic mobility measurements were performed at $\theta = 12.8^\circ$ using the M3-PALS (Phase Analysis Light Scattering) technique to detect the particle movement, which is used to calculate its electrophoretic mobility and from which the ζ -potential of the nanoparticles can be estimated. The samples were put in disposable polystyrene cuvettes of 1 cm optical path length with Milli-Q water as solvent and the two types of measurements were thereafter conducted one after another (DLS first). The hexosome nanoparticle samples were diluted 1:100

times prior to the measurements. The measured time correlation functions of the scattered intensity were analyzed using the software available in the Malvern instrument to obtain the intensity-weighted size distributions based on the apparent hydrodynamic diameter, d_H , which is calculated from the Stokes-Einstein relation $d_H = kT/3\pi\eta_0D$, where D is the translational collective diffusion coefficient, obtained from the decay time of the correlation function, and η_0 is the viscosity of water. The reported nanoparticle size values correspond to an average of between three to five measurements.

Small-Angle X-ray Scattering (SAXS)

The SAXS measurements were performed at MAX-lab, Sweden, using the SAXS beamline I911-4.⁸ The hexosome dispersions were injected in quartz capillary cells. The sample cell was mounted in thermostated holder at a distance of 1952 mm from the 1M PILATUS 2D detector. The q calibration was done using a silver behenate standard sample. The x-ray wavelength was 0.91 Å and the size of the beam at the sample was approximately 0.25 x 0.25 mm. Diffractograms of the dispersions were recorded at each temperature during 3 minutes. The intensities recorded by the 2D detector were integrated using Fit2D provided by A. Hammersley. (<http://www.esrf.eu/computing/scientific/FIT2D/>)

Photophysical characterization

Hexosome dispersions were diluted with Milli-Q water (1:30) before performing the photophysical measurements. The emission and excitation spectra were recorded with a Perkin Elmer LS 55 spectrofluorimeter. The fluorescence quantum yield on Py-BODIPY in different solvents was determined by using Rhodamine 6G dissolved in EtOH as the reference standard ($\Phi_{ref} = 0.94$). The absorption spectra were recorded on a Thermo Nicolet Evolution 300 spectrophotometer.

Cell culture and treatments

HeLa cells (ATCC collection) were grown in phenol red-free Dulbecco's modified Eagle's medium (DMEM, Molecular Probes, USA) with high glucose, supplemented with 10% (v/v) fetal bovine serum, penicillin (100 U mL⁻¹) and streptomycin (100 µg mL⁻¹) (Invitrogen) in 5% CO₂ incubator at 37 °C. For live cell imaging, cells were seeded in 35 mm dishes and experiments were carried out two days after seeding when cells had reached 90 % confluency. Empty or dye loaded nanoparticles were added to the cells at a concentration of 1: 500 (2 µL in 1 mL of fresh medium) and incubated at 37 °C for 4 h. Fresh serum-free medium was used to remove the extracellular particle suspension before imaging session. For the colocalization experiments, cells were grown on glass coverslips, incubated with Py-BODIPY loaded nanoparticles for 4 h, fixed in 4% paraformaldehyde (PFA) in phosphate-buffered saline (PBS) for 10 min and washed three times with PBS. Cells were then stained with HCS LipidTOx Red Neutral lipid Stain (1:200, Molecular Probes, USA) in PBS for 45 min and images were directly acquired at 40x without wash steps.

Fluorescence microscopy

Light microscopy observations were made using a Zeiss (Axioskop) upright fluorescence microscope (Zeiss, Oberkochen, Germany) equipped with 10x, 20x and 40x/0.75 NA water immersion objectives and a HBO 50 W L-2 mercury lamp (Osram, Berlin, Germany). Twelve-bit-deep images were acquired with a monochrome cooled CCD camera (QICAM, Qimaging, Canada). For observation of Py-BODIPY, filters were: ex 470 ± 20 nm, em 535 ± 40 nm; LipidTOX ex 546 ± 6 nm, em 620 ± 60 nm. Digital images were analyzed and image alignments were obtained with Image Pro Plus software (Media Cybernetics, Silver Springs, MD).

Cytotoxic activity: MTT assay

The cytotoxic effect of nanoparticle formulations was evaluated in HeLa cells by the MTT assay. HeLa cells were seeded in 24-well plates at density of 3×10⁴ cells/well in 500 µL of serum-containing media. Experiments were carried out two days after seeding when cells had reached 90%

confluence. Empty or dye loaded nanoparticles were added to the cells at concentrations of 1:500 (2 μ l in 1 mL of fresh medium) and incubated at 37 °C for 4 h. A 50 μ L portion of MTT solution (3-(4,5-dimethylthiazol-2-yl)-2,5-diphenyltetrazolium bromide) (5 mg/mL in H₂O) (Sigma-Aldrich, St Louis, MO, USA), was then added and left for 2 h at 37 °C. The medium was aspirated, 500 μ L of DMSO was added to the wells, and color development was measured at 570 nm with an Infinite 200 auto microplate reader (Infinite 200, Tecan, Austria). The absorbance is proportional to the number of viable cells. All measurements were performed in quadruplicate and repeated at least three times. Results are shown as percent of cell viability in comparison with non-treated control cells. Statistical analysis was carried out with Graph Pad INSTAT software (GraphPad software, San Diego, CA) and statistically significant difference was evaluated by one-way analysis of variation (One-way ANOVA) and the Bonferroni post Test.

Table S1. Selected bond lengths (\AA), angles ($^\circ$), dihedral τ ($^\circ$) optimised at DFT level for Py-BODIPY. The excitation energy E (eV) and oscillator strength f calculated at TDDFT level for the two electronic transitions at the lowest energy are also reported.

	Gas phase	MeOH	EtOH	MeCN	DMF	DMSO	DCM	EtOAc	Toluene	Acetone	Hexane
B-N	1.559	1.547	1.547	1.547	1.547	1.547	1.548	1.549	1.553	1.547	1.554
B-F	1.388	1.401	1.400	1.401	1.401	1.401	1.398	1.398	1.394	1.400	1.393
N-B-N	105.49	106.38	106.37	106.38	106.38	106.39	106.27	106.21	105.93	106.35	105.83
F-B-F	110.90	109.11	109.14	109.10	109.10	109.09	109.33	109.47	110.01	109.16	110.22
N-B-F	110.12	110.45	110.44	110.44	110.45	110.23	110.27	110.37	110.06	110.43	110.24
τ	68.00	68.46	65.52	68.47	68.47	68.49	67.46	68.87	69.14	68.58	69.12
E_1	2.383	2.196	2.198	2.195	2.194	2.227	2.215	2.228	2.279	2.232	2.302
f_1	0.027	0.034	0.035	0.034	0.036	0.035	0.036	0.035	0.038	0.034	0.036
E_2	3.103	2.991	2.983	2.987	2.966	2.978	2.969	2.982	2.956	2.992	2.984
f_2	0.360	0.448	0.456	0.452	0.472	0.477	0.473	0.463	0.495	0.464	0.470

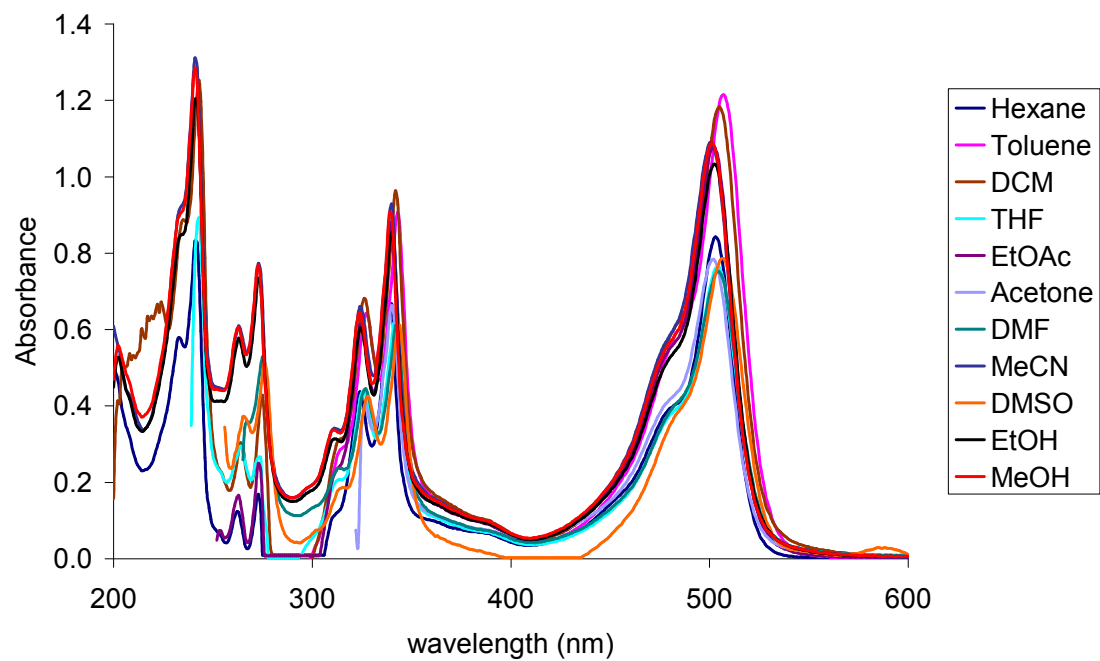


Fig. S1. Absorption spectra of Py-BODIPY in different solvents. [Py-BODIPY] = $2.5 \cdot 10^{-5}$ M.

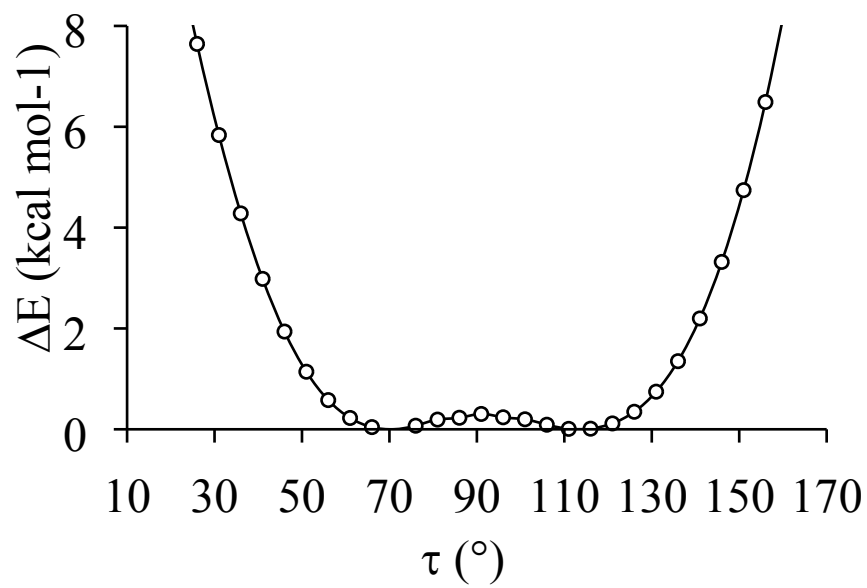


Fig. S2. Relative variation of the total electronic energy ΔE as a function of the rotation (τ) of the pyrene pendant in Py-BODIBY calculated in the gas phase at DFT level.

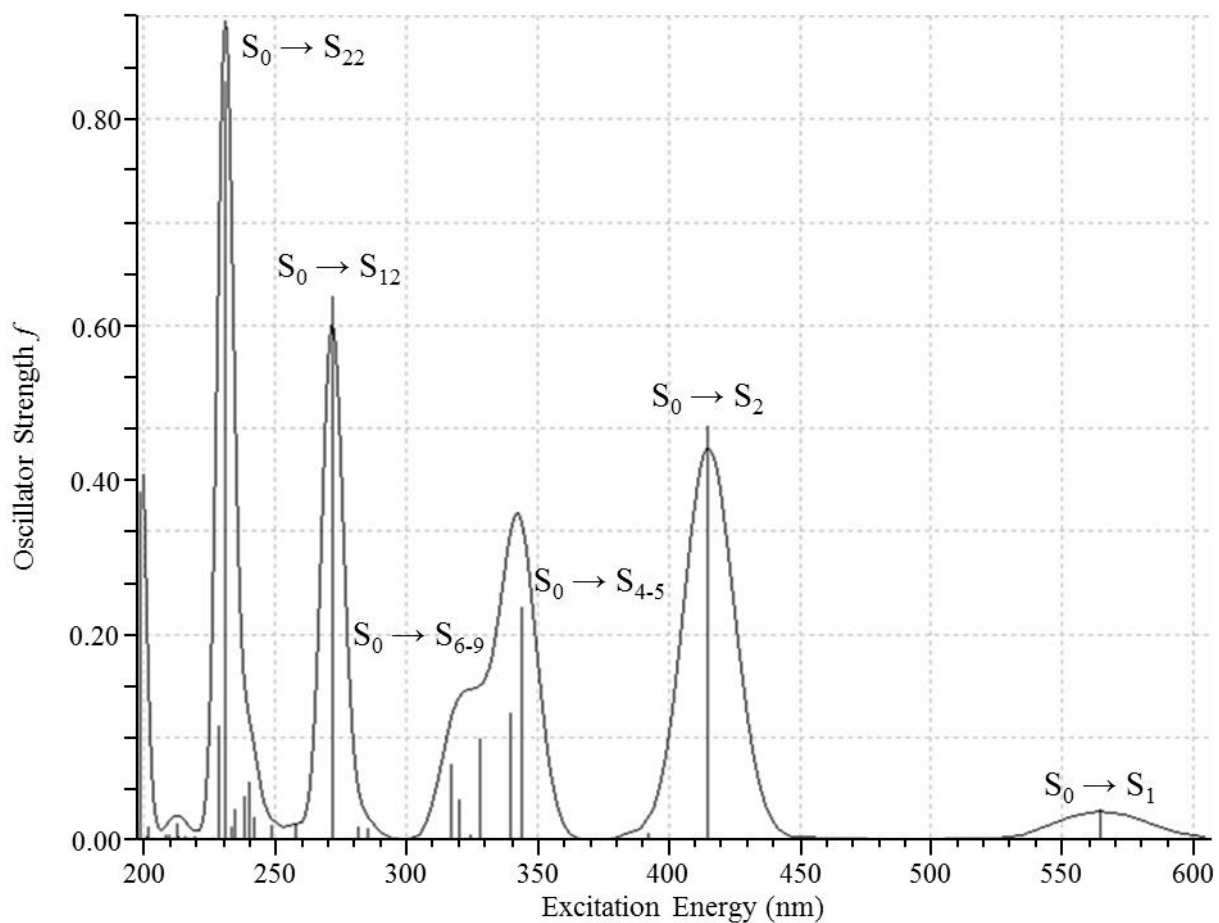


Fig. S3. Simulated UV-Vis excitation spectrum calculated at TDDFT level for Py-BODIPY in MeCN. Peak half width at half height 0.10 eV.

References

1. Gaussian 09, Revision A.02, M. J. Frisch, G. W. Trucks, H. B. Schlegel, G. E. Scuseria, M. A. Robb, J. R. Cheeseman, G. Scalmani, V. Barone, B. Mennucci, G. A. Petersson, H. Nakatsuji, M. Caricato, X. Li, H. P. Hratchian, A. F. Izmaylov, J. Bloino, G. Zheng, J. L. Sonnenberg, M. M. Hada, M. Ehara, K. Toyota, R. Fukuda, J. Hasegawa, M. Ishida, T. Nakajima, Y. Honda, O. Kitao, H. Nakai, T. Vreven, J. Montgomery, J. A., J. E. Peralta, F. Ogliaro, M. Bearpark, J. J. Heyd, E. Brothers, K. N. Kudin, V. N. Staroverov, R. Kobayashi, J. Normand, K. Raghavachari, A. Rendell, J. C. Burant, S. S. Iyengar, J. Tomasi, M. Cossi, N. Rega, J. M. Millam, M. Klene, J. E. Knox, J. B. Cross, V. Bakken, C. Adamo, J. Jaramillo, R. Gomperts, R. E. Stratmann, O. Yazyev, A. J. Austin, R. Cammi, C. Pomelli, J. W. Ochterski, R. L. Martin, K. Morokuma, V. G. Zakrzewski, G. A. Voth, P. Salvador, J. J. Dannenberg, S. Dapprich, A. D. Daniels, Ö. Farkas, J. B. Foresman, J. V. Ortiz, J. Cioslowski and D. J. Fox, Gaussian, Inc., Wallingford CT, Edition 2009.
2. C. Adamo and V. Barone, *Journal of Chemical Physics*, 1999, **110**, 6158-6170.
3. M. J. Frisch, *GAUSSIAN 09 User's Reference*, Gaussian, Inc., Pittsburgh, PA, 1998.
4. R. Ziessel, C. Goze, G. Ulrich, M. Césarío, P. Retailleau, A. Harriman and J. P. Rostron, *Chemistry - A European Journal*, 2005, **11**, 7366-7378.
5. J. Tomasi, B. Mennucci and R. Cammi, *Chemical Reviews*, 2005, **105**, 2999-3093.
6. G. Schaftenaar and J. H. Noordik, *Journal of Computer-Aided Molecular Design*, 2000, **14**, 123-134.
7. GaussView, Version 5, R. Dennington, T. Keith and J. Millam, Semichem, Inc., Shawnee Mission, KS, 2009.
8. A. Labrador, Y. Cerenius, C. Svensson, K. Theodor and T. Plivelic, *Journal of Physics: Conference Series*, 2013, **425**, 072019.